

Investigating the Role of Aggrecan in Intervertebral Disc Degeneration

Undergraduate Honors Engineering Research Thesis for Biomedical Engineering

Biomedical Engineering Department of The Ohio State University

By Brian King

The Ohio State University

2018

Dr. Purmessur-Walter, Advisor

Abstract

Low back pain affects nearly 85% of the population of the United States, and is associated with a huge socioeconomic burden. One of the leading causes of low back pain is Intervertebral Disc (IVD) degeneration, which results in an ingrowth of blood vessels and neurites, as well as a sensitization of those neurites. Previous research has indicated that both Aggrecan plays a role in regulating angiogenesis in the IVD, and Aggrecan has also been shown to inhibit neurogenesis and sensitize neurites. However, it is unclear which components of Aggrecan control its inhibitory effects. The goal of this study was to determine how intact and degraded Chondroitin Sulfate groups, the dominant side-chains of Aggrecan, affect angiogenesis in vitro, as well as the sensitization of neurites. Human Umbilical Vein Endothelial Cells (HUVECs) were cultured with either intact or degraded Chondroitin Sulfate-A (CSA), Chondroitin Sulfate-B (CSB), or Chondroitin Sulfate-C (CSC) at a concentration of either 10 $\mu\text{g/ml}$ or 100 $\mu\text{g/ml}$ for 16 hours during a tubular formation assay. The tubular assay was quantified for total tubular length using the Angiogenesis Analyzer plugin for Image J. The assay showed that no inhibition occurred for any of the groups, and that pro-angiogenic effects were observed for the 100 $\mu\text{g/ml}$ concentration of degraded CSC. The protocol developed to investigate the effect of Aggrecan on neurite sensitization involved optimizing the methodology for extracting Dorsal Root Ganglia (DRGs) cells from mice for use as a primary cell model. The protocol developed is based on literature, but optimizes for simplicity, time, and reduction in the cost of surgical instruments. This protocol achieves these goals, and attains high viability for DRG cell clusters, but fails to consistently retrieve viable cells from the intact DRGs. This study sought to investigate the role chondroitin sulfate side chains play in angiogenesis, and it found evidence that the degraded factors can have pro-angiogenic effects. The study also sought to

develop a protocol that could be used to aggregate in the role of sensitization, and it improved the speed and simplicity of existing procedures.

Acknowledgements

I would like to thank Dr. Purmessur for her continued guidance, support, and understanding as I completed this project. I would like to thank Taylor Yeator and Pavel Sul for their Mentorship and support, as well as contributing to my initial success. I would like to thank Katie Latskins and Nina Tang for helping me sort through the endless problems associated with optimization, and for contributing to a constructive work environment. I would also like to thank the rest of the Spinal Therapeutics Lab for their part in making it such a great place to work.

I would like to thank Dr. Litsky for sitting in on my Defense Committee and providing Orthopaedic insight.

I would like to thank the Ohio State University's department of Engineering for their trust in my project and their financial support of the project, which allowed me to have resources for my project that would otherwise be impossible.

Table of Contents

Contents

Abstract	ii
Acknowledgements	iv
List of Figures	vii
Introduction	1
Anatomical Review	1
Unhealthy Intervertebral Disc Microenvironment	2
Aggrecan as a Potential Mechanism for Neurovascular Ingrowth	3
Relevance	4
Specific Aims and Hypotheses	4
Methodology	5
Angiogenesis Experiments	5
Cell Culture	5
Aggrecan Source	5
Aggrecan Degradation	5
Experimental Media Conditions	6
HUVEC Angiogenesis Assay	6
Image Collection	7
Image Analysis	7
Statistical Analysis	8
Protocol Development	9
Cited Protocols	9
Animal Information	9
Gross Dissection and Spinal Column Isolation	10
Microscopic Dissection and DRG Removal	12
Enzymatic Digestion	13
Results	13
DMMB Results	13
Angiogenesis Experiments	14
Protocol Development	16
Discussion	17

Angiogenesis Experiments.....	17
Protocol Development.....	18
Significance and Conclusions.....	19
Limitations and Future Work.....	19
DRG Cell Viability.....	19
Angiogenesis Assay	19
Future Work.....	20
References.....	21

List of Figures

Figure 1: Anatomy of the Intervertebral Disc ⁶	1
Figure 2: Structure of Aggrecan ¹⁹	3
Figure 3: HUVEC Tubular Assay Representative Images	7
Figure 4: Pixelized version of HUVEC Tubular Formation	8
Figure 5: Gross Mouse DRG Dissection	11
Figure 6: DRG Microscopic Dissection	12
Figure 7: DMMB Quantification	14
Figure 8: Representative Tubular Assay Images	14
Figure 9: Controls for Tubular Assay Well Plates	15
Figure 10: Live-Dead for a Whole DRG Cell Clump	16
Figure 11: DRG cell count using Hemocytometer	16

Introduction

Lower back pain affects nearly 85% of people in the United States at some point in their lives¹, and results in a significant social and economic burden². Degeneration of the intervertebral disc (IVD) has been implicated in its development, but its mechanisms are still not fully understood³. Intervertebral disc disease severely weakens the structure of the disc, and often leads to disc herniation⁴. Disc herniation, or a pressing of disc tissue onto adjacent sensory nerves, is one of the main causes of the pain associated with the disease⁵. However, many patients experience intense pain associated with the disease in the absence of herniation. In these cases, angiogenesis, or ingrowth of blood vessels, as well as ingrowth of nerves, neurogenesis, are commonly reported³. It is this component of intervertebral disc disease that this paper will examine.

Anatomical Review

A healthy IVD contains several important components that contribute to its functionality as seen in Figure 1, below.

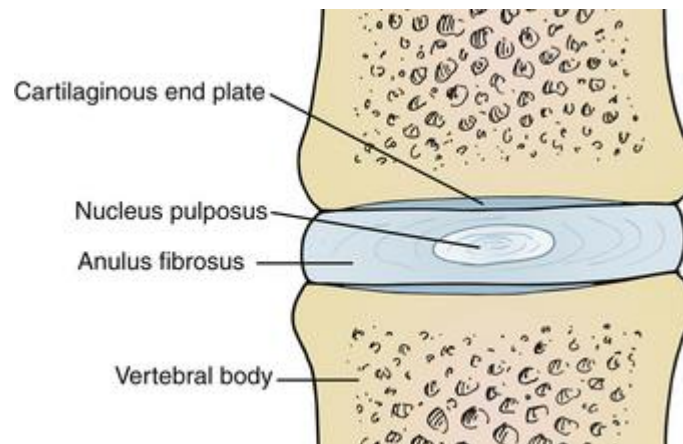


Figure 1: Anatomy of the Intervertebral Disc between two vertebral bodies⁶

The core of the IVD is the Nucleus pulposus (NP), which consists of elastin and collagen II fibers contained in a hydrated Aggrecan-containing gel. The proteoglycans present in this region make up approximately 15% of its wet weight while the remaining majority space contains water.⁷ This water is drawn into the disc via Aggrecan, which maintains a high osmotic pressure in order to keep the cushion-like nature of the disc⁸. The NP contains few cells, with a low density of chondrocyte-like cells⁹. In a healthy disc, no blood vessels or nerves are present, and nutrition stems entirely from diffusion.

Outside the NP is the Anulus Fibrosus (AF) region, which has a similar makeup to the NP, but has a much higher collagen concentration. Collagen fibers provide the structure necessary for its lamellar structure, and provide substantial strength⁷. Cells in this region tend to be more fibroblast-like, yet blood vessels and nerves are still not typical of the native environment, and again nutrition comes from diffusion.

The Cartilaginous endplate separates the disc from the adjacent vertebral bodies, and is generally highly porous and somewhat vascularized to allow for nutritional supply to the rest of the disc¹⁰. Nociceptive nerves terminate in this region and do not penetrate the disc itself in healthy disc tissue.⁷

Unhealthy Intervertebral Disc Microenvironment

When Intervertebral Disc Degeneration (IVDD) manifests, the biochemical and cellular makeup of the disc substantially changes. The matrix degrades as a result of an upregulation of inflammatory cytokines. One of the main targets of this degradation is Aggrecan, and as a result the disc loses significant hydrostatic pressure¹¹. In addition, resulting from the degradation, the normally aneural and avascular IVD is penetrated by both nociceptive nerve fibers³ and blood vessels¹². Sensitization of neurites has also been observed as a result, and is of significant note.

Aggrecan as a Potential Mechanism for Neurovascular Ingrowth

As mentioned, Aggrecan, an important structural proteoglycan in the disc, degrades in IVDD. While this proteoglycan primarily controls the hydration of the disc, it also has been shown to have an important role in regulation of neurovascular ingrowth. Presence of Aggrecan has been shown to inhibit nerve ingrowth into the intervertebral disk^{13,14}, and its degradation in degenerative IVDs indicates it is highly important to degenerative disc disease¹⁴. Aggrecan has also been shown to inhibit angiogenesis, the penetration of blood vessels into the normally avascular disc¹⁵. Aggrecan contains both a core protein, and a series of side-chains, see Figure 2 below.

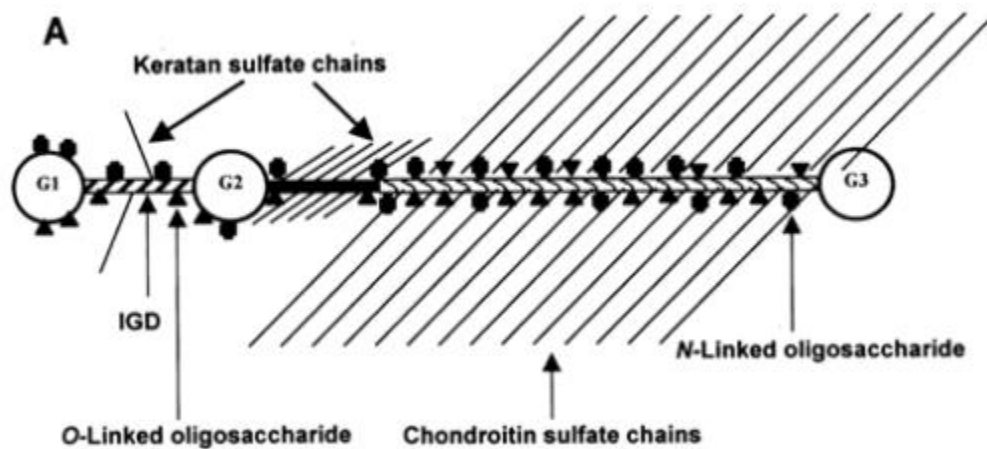


Figure 2: Structure of Intact Aggrecan¹⁶

Human Aggrecan has a variety of molecular side-chains that, while intact, could contribute to the inhibition of angiogenesis including: 0S iduronic acid, 4S galactosamine, and 6S galactosamine¹⁷. Both these side-chains and the Aggrecan core protein degrade in a degenerate disc. Previous research has indicated that intact Aggrecan with attached side chains has an inhibitory effect¹⁸, but whether this is due to the core or those side chains is unclear. The specific mechanism of inhibition for neurovascular ingrowth is an important detail to determine.

Previous research has also demonstrated that relative concentration of Chondroitin – 6 -Sulfate increases with age in bovine tissue for both the AF and the NP compared to Chondroitin – 4 -Sulfate, and Chondroitin – 0 -Sulfate, which together make up the majority of the Chondroitin Sulfate side-chain composition¹⁹. Because there is a difference between the relative abundance of the different Chondroitin Sulfate groups for different ages in Bovine tissue, it could provide some insight into how the relative groups affect angiogenesis. In addition, degraded side-chains and core monomer could provide the necessary materials necessary for neurovascular growth, and could actually be aiding in the ingrowth of blood vessels and nerves.

Relevance

Investigating the mechanisms for the processes of neurovascular ingrowth and sensitization in IVDD, which are not fully understood, could result in better long-term treatment for the disease. If this project can determine which specific chondroitin sulfate side-chain of Aggrecan is having the inhibitory effect on neurovascular ingrowth, targeted treatment can be developed that can prevent or reverse these processes. In addition, determining the specific factors that affect the sensitization of neurites in IVD disease could result in the development of treatments that reduce the pain associated with this effect.

Specific Aims and Hypotheses

Aim 1: To determine how degraded Aggrecan products will affect the growth of blood vessels.

We hypothesize that intact Aggrecan side-chains will inhibit angiogenesis, while degraded side-chains will aid in angiogenesis.

Aim 2: To develop a protocol that will allow our lab to isolate mouse dorsal root ganglia (DRGs) for use in determining how Aggrecan affects neurite sensitivity.

Methodology

Angiogenesis Experiments

Cell Culture

Human Umbilical Vein Endothelial Cells (HUVECs, Cascade Biologics, C-015-5C) were cultured in Phenol red-free media (Gibco M200PRF500) supplemented with 1% Penn-Strep (Gibco 15140-122) and 2% Low Serum Growth Supplement (Cascade Biologics, S-003-10). They were grown inside of plastic culture flasks (VWR Tissue Culture Flasks 10062-864) at 37°C with 5% CO₂ in an incubator (OASIS). The cells were passaged when they reached 70-90% confluency.

Aggrecan Source

To study the effect of Aggrecan on angiogenesis, we used a series of commercially available Aggrecan sources which modeled the side-chains present in human Aggrecan. Chondroitin Sulfate-A (CS-C0) contains a high amount of Chondroitin-6-Sulfate, which can be used to model 6S Galactosamine. Chondroitin Sulfate-B (CS-B) contains a high amount of dermatan-4-sulfate, which can be used to model 4S Galactosamine. Chondroitin Sulfate-C (CS-A) contains high amounts of Chondroitin-4-Sulfate, which contains a high amount of 0S glucuronic acid. Each Chondroitin Sulfate side chain derives from shark due to its similarity to its human analog, and its ease of access. 10.0 mg/mL stock concentrations were made for each Aggrecan side chain (CSA, CSB, CSC) by dissolving side chain solid in sterile H₂O at a ratio of 10 mg per mL. All stock solutions were aliquoted into 1 ml aliquots and stored in a -20°C freezer.

Aggrecan Degradation

To create the degraded Aggrecan necessary for experiments, 50ul of Chondroitinase-ABC was used per 10 ml media at the desired concentration. This media was then sterile filtered using a 0.2 µm pore-sized filter due to the non-sterility of the commercial Chondroitinase-ABC. To create the desired concentration of Chondroitinase-ABC, 5 units of Chondroitinase-ABC (Chondroitinase ABC from

Proteus Vulgaris, C3667-5UN) was suspended in a solution of 0.5mL of 1M TRIS, .0490g sodium acetate, .002g BSA, and 9.5 ml of H₂O.

To test the efficacy of the degradation of Chondroitin using Chondroitinase-ABC, a Dimethyl-Methylene Blue (DMMB) assay was used to quantify the amount of intact chondroitin sulfate present for both intact and degraded samples of chondroitin sulfate of the same concentration.

Experimental Media Conditions

All conditioned media contained Medium 200 phenol red free + 100U/ml penicillin-100 µg/ml streptomycin + low serum growth supplement. Media was generated with 10µg/ml or 100µg/ml of intact or degraded Chondroitin Sulfate, for each side chain, CSA, CSB, or CSC. Degraded media was created by first creating twice the necessary volume of the corresponding concentration of intact media. This media was then split, and Chondroitinase-ABC was added to half, as described in the previous section.

HUVEC Angiogenesis Assay

HUVEC functional angiogenesis assays are a way to quantify an otherwise in vivo process on a surface in vitro. To perform this assay, HUVECs were expanded to 80% confluency at a passage of less than 10. While the cell line is immortalized, HUVECs sometimes exhibit a change in morphology given enough proliferation in vitro. After thawing Geltrex basement membrane (Gibco, A14132-02) overnight, 100µl was added to each well of a 24 – well plate, keeping the Geltrex on ice. The plates were then put in a 37°C incubator for 30 minutes to gel. HUVECs were then trypsonized and resuspended in their respective media conditions. 6 different conditions were used, including the positive and negative control, with four experimental replicates for each condition. The positive control consisted of Medium 200 phenol red free + 100U/ml penicillin-100 µg/ml streptomycin + 1 ml low serum growth supplement per

200 ml phenol red free media. Negative control was the same recipe, but lacked low serum growth supplement. Cells were grown for 16 hours before imaging.

Image Collection

Fluorescent images were taken at a magnification of 4x using a Nikon elipse Ti microscope. 5 images were randomly taken per well utilizing the automated imaging software associated with the microscope, for a total of 120 images. The images were converted to 8 bit, mono-image tiffs and exported for further analysis.

Image Analysis

Images were first blinded using a blinding batch file to avoid bias, and then each image was subsequently analyzed for areas of excessive overgrowth of cells. These areas impact the ability of the software to complete its analysis and were removed from the image pool. Examples of images that would be included and excluded can be found below in Figure 3.

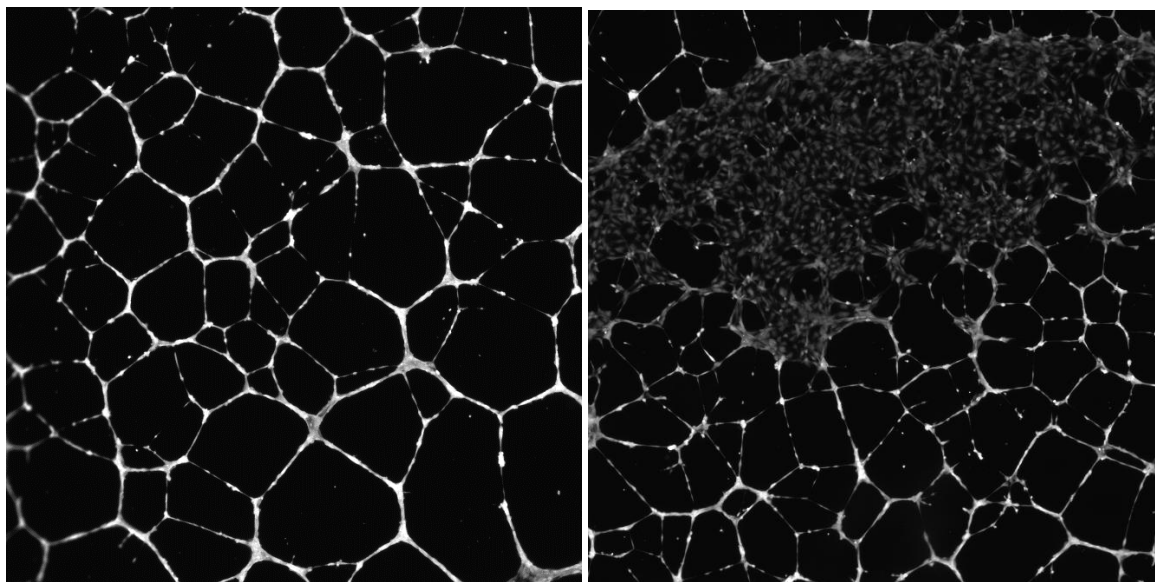


Figure 3: HUVEC Tubular Assay Representative Images. (Left) Included in image analysis while (right) removed.

The remaining images were analyzed for total tubule length using Angiogenesis Analyzer plugin for Image J²⁰. This software quantifies the networks total tubule length through creation

of a pixelized version of the network. To create this pixelized network, “three iterations were performed with minimum object size set at 50 pixels, minimum branch size at 25 pixels, artifactual loop size at 1000 pixels, isolated element threshold at 100 pixels and master segment threshold at 30 pixels”, as done by Marquez-Curtis et al.²¹ An example of a pixelized network can be found in Figure 4, below.

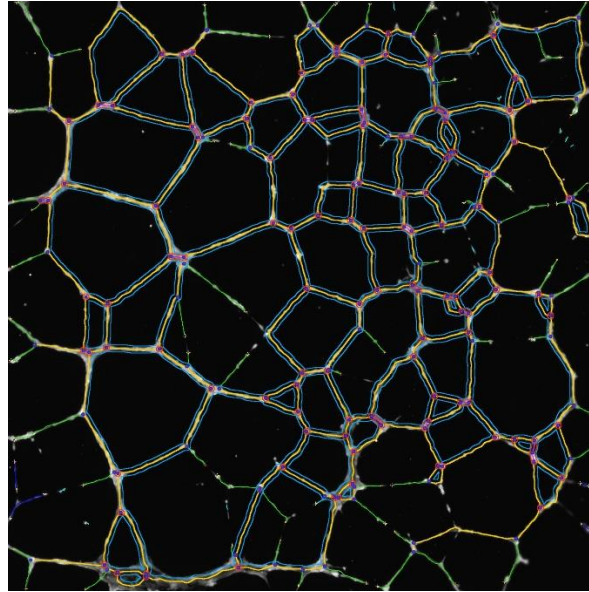


Figure 4: Pixelized version of HUVEC Tubular Formation

The program outputs a variety of data, but the data of interest was total tubular formation due to its indication of general angiogenesis. Tubular formation data was then unblinded and further analyzed.

Statistical Analysis

Statistical Significance was determined using GraphPad Prism version 6 software. Kruskal Wallis nonparametric test was used with Dunn’s post-hoc analysis for each experiment. A one-tailed t-test was utilized to determine significance between the controls with LSGS(Positive) and the controls without LSGS(Negative). Significance was established if $p < .05$. In each case, experimental n was between 3 and 4.

Protocol Development

Cited Protocols

The dissection component of this protocol is derived from the protocol developed by James N. Sleight et al²² for rapid isolation of mouse dorsal root ganglia. This protocol is mostly developed, but aspects of this protocol needed to be re-optimized for this lab and described in a higher level of detail. Specifically, the microscopic dissection and removal of DRGs needed additional clarity, which will be addressed in this paper.

The enzymatic digestion protocol component of this lab is derived from a protocol developed by Dr. Popovich's lab at The Ohio State University, and similarly requires additional optimization for its use in our lab.

Animal Information

The mice utilized for the optimization of this protocol were Wild-Type adult males, and were grown and cared for in the OSU Laboratory Animal Resources building as training animals. All animals were euthanized with CO₂ gas, with the secondary form of euthanasia being heart puncture. Mice were euthanized immediately prior to dissection to improve the viability of the DRGs to be dissected.

Gross Dissection and Spinal Column Isolation

Following euthanasia, the animal is sprayed with 70% ethanol to reduce contamination and reduce hair interfering with the dissection tools (Fig. 5b). An incision through the skin and fur should then be made down the center of the dorsal side of the mouse, revealing the underlying muscle beneath (Fig. 5c). Following this, an incision is made close to the lower hips of the mouse and should be continue up both sides of the spinal column, with the goal of separating the spinal column from the rest of the mouse. The connective tissue between the viscera and the spinal column should also be severed, with care taken to ensure the DRGs are not damaged. Once the incisions have made it up to the neck, the spinal column can be severed at the base of the neck and removed from the body of the mouse (Fig. 5d).

Once the spinal column is removed, the soft tissue along the sides of the spinal column can be removed using small surgical scissors (Fig. 5e). Care should be taken to ensure that the spinal column is dorsal side up, to protect the DRGs. The spinous processes can then be revealed using a scalpel blade to separate out the soft tissue to make the spinal column cut easier (Fig. 5f). At this point, the spinal column can be cut vertically down the center, with care being taken to cut directly in the center of the spinous process (Fig. 5g). Deviance to one side or the other can result in a loss of yield of DRGs. Once the spinal column is cleaved, the spinal column should be placed under a dissecting microscope.

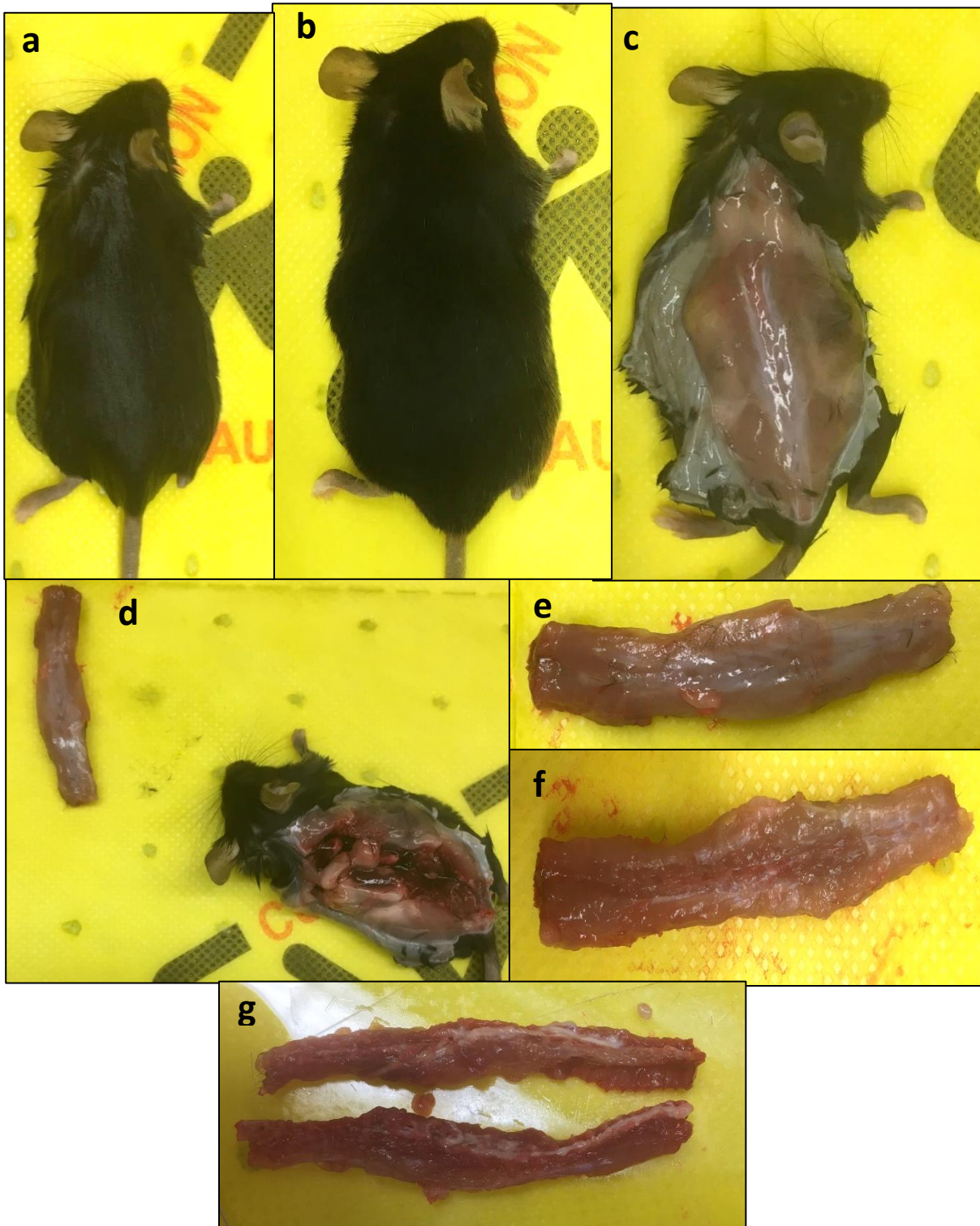


Figure 5: Gross Mouse DRG Dissection

(a) Lay the mouse dorsal side up (b) Spray with 70% ethanol (c) Remove the skin and fur from the area dorsal to the spinal column (d) Remove the spinal column from the mouse (e) Remove the excess soft tissue from the sides (f) Scrape the tissue off the spinous processes to make the separation easier (g) Cut the spinal column in half vertically using a scalpel

Microscopic Dissection and DRG Removal

When each half of the spinal column is placed under the dissecting microscope, the spinal cord is clearly visible (Fig. 6a). This should be moved to the side using a small pair of forceps to reveal the DRGs which are located underneath the spinal cord (Fig. 6b). Each DRG is visible in its own socket, and has connections to the spinal cord, and afferents that extend into the socket. However, each DRG is covered by a layer of meninges that needs to be removed (Fig. 6c). A small pair of scissors should be used to “scoop” out the DRG by severing the afferents that extend into the socket, with care taken not to pinch the DRG as that will induce an injured phenotype (Fig. 6d).

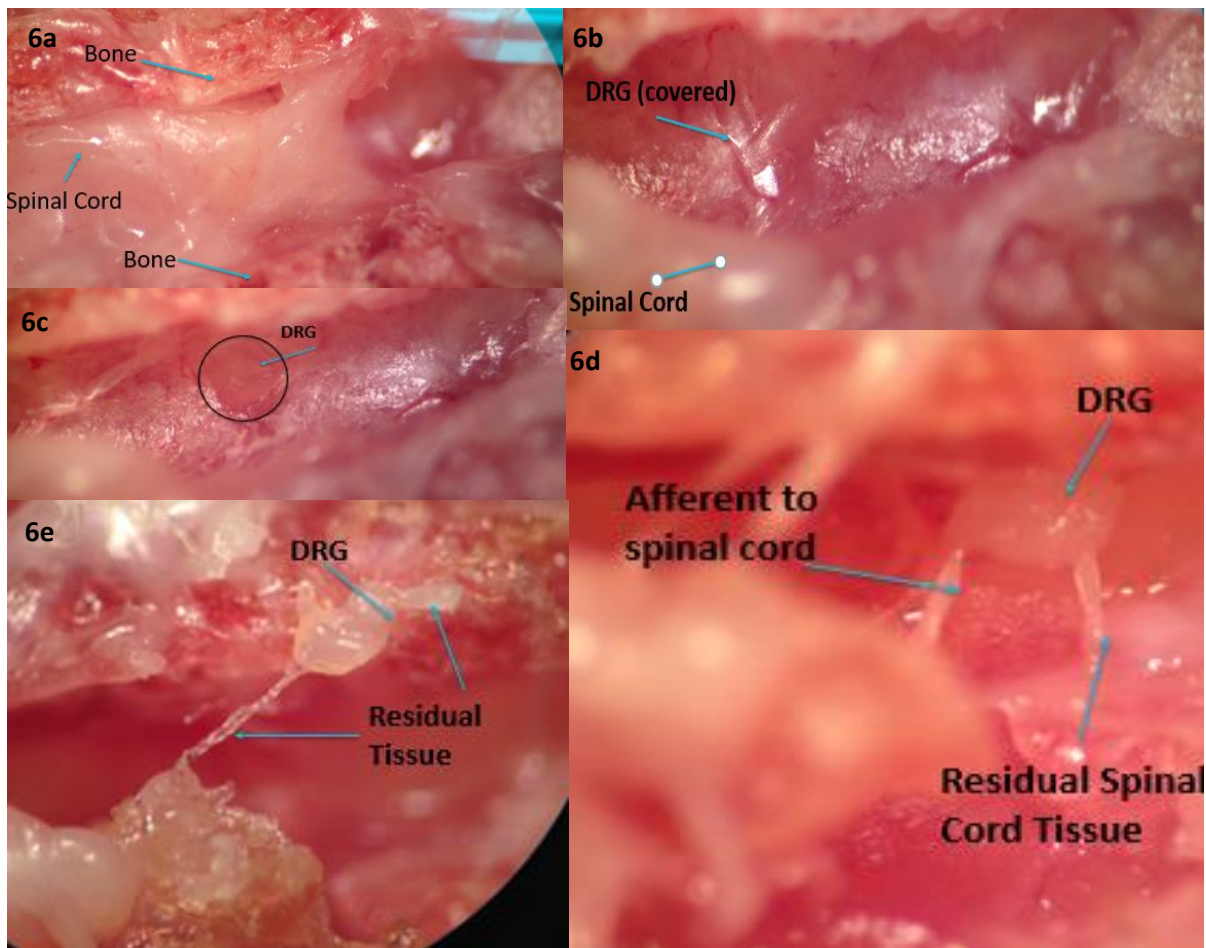


Figure 6: DRG Microscopic Dissection

(a) Place one half of the spinal column under the dissection microscope, dorsal side up (b) Remove the spinal cord from covering a DRG (c) Remove the meninges (d) Remove the DRG from its socket (e) Remove the remaining axons from the DRG

Once the DRG is scooped out, it can be picked up by an axon bundle, and the remaining connections can be cut (Fig. 6e). Once the connections are cut, the DRG should be placed in ice cold HBSS for the subsequent enzymatic digestion step.

Enzymatic Digestion

Following DRG isolation, the intact DRGs are washed with HBSS to remove blood cells, and then enzymatically digested using Dispase(5U/mL) and Collagenase II(200U/mL) for 45 minutes at 37°C. The cells are then washed again with warm HBSS, and then treated with DNase to prevent free DNA from compromised cells that may affect DRG viability. The intact DRGs are then triturated vigorously with a pipette for 15 pumps, before the supernatant is removed. The supernatant contains the free cells in suspension, and continuing to triturate these results in substantial cell death. The remaining cell clumps are then triturated again for another 20 pumps to break them up. The resulting suspension and the supernatant are then passed through a 40µm cell filter to remove residual debris. The resulting cells are counted utilizing a hemocytometer.

Results

DMMB Results

The amount of Chondroitin Sulfate present in the intact and degraded samples of CSA, CSB, and CSC was quantified relative to a standard curve from 0 to 250 µg/ml of Chondroitin Sulfate-A. The results of this analysis can be found in Figure 7.

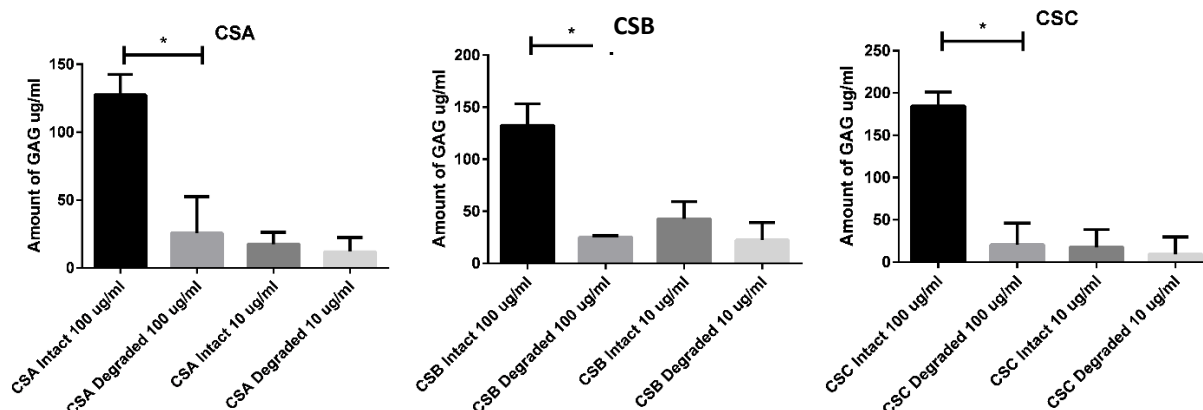


Figure 7: DMMB Quantification

In each group, the intact group at the higher concentration had significantly higher GAG concentration than the degraded group. This shows that the degradation protocol was effective, and our Chondroitinase- ABC was able to effectively degrade the Chondroitin Sulfate side-chains.

Angiogenesis Experiments

A HUVEC angiogenesis assay was ran for each condition as previously described, and images were collected 16 hours after the commencement of the assay. Representative images are displayed below in Figure 8.

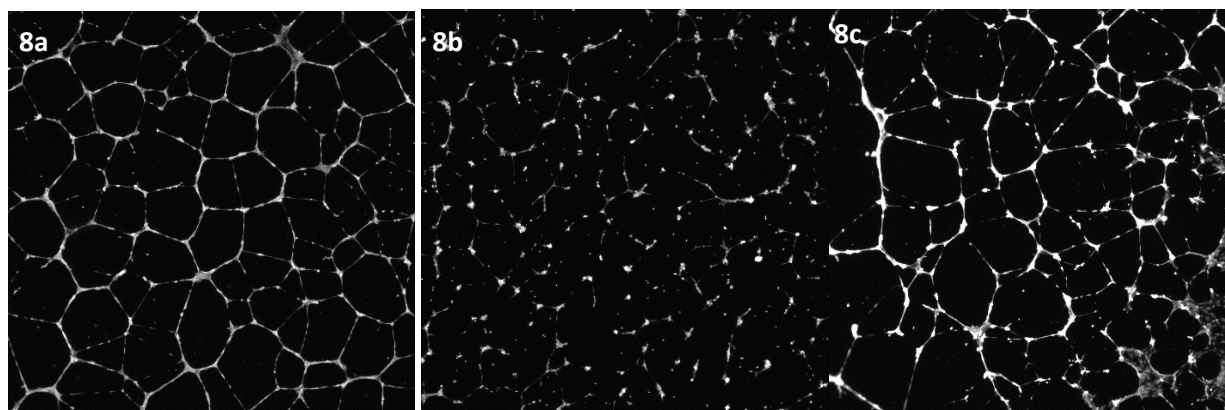


Figure 8: Representative Tubular Assay Images

(a) Positive Control from CSA well plate (b) Negative Control from CSA well plate (c) CSC 100 μ g/ml

To demonstrate that the tubular formation protocol was working, controls with both LSGS (positive control) and without LSGS (negative control) were quantified and analyzed. The controls were used to verify that the assay worked for each of the titled groups, as shown below. In each condition, the significant difference between the positive control and the negative control indicated that the assay was successful. Post assay verification, all data was quantified and compared to their respective positive controls, as shown in Figure 9 below.

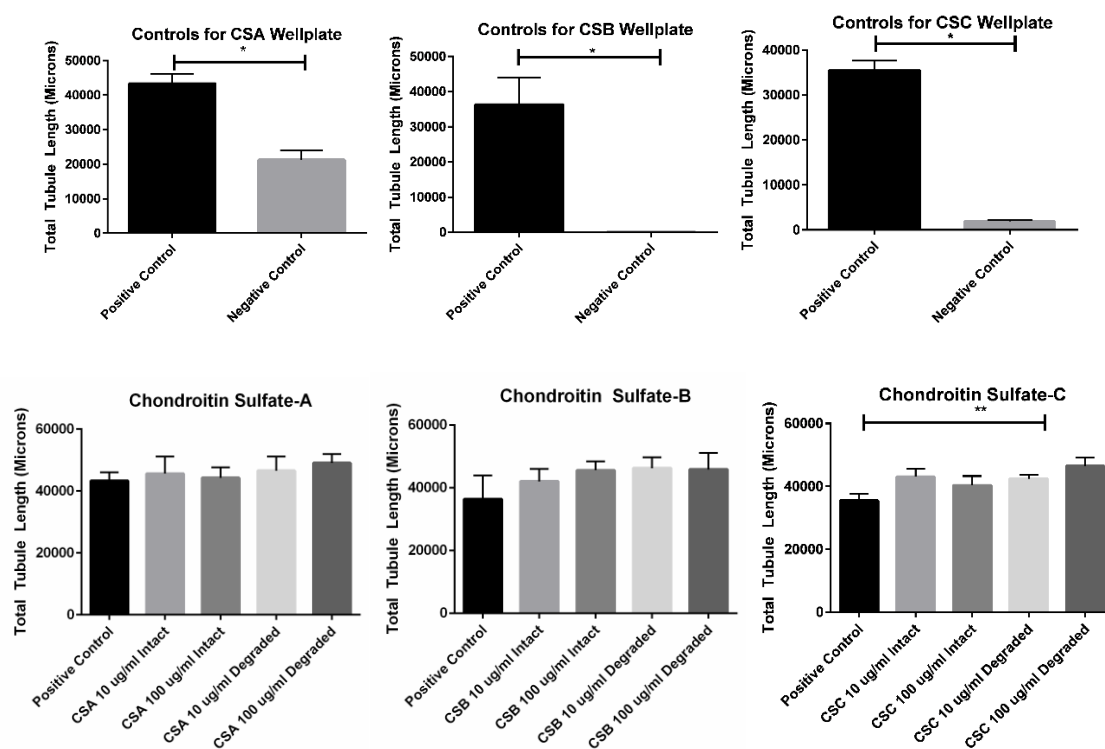


Figure 9: HUVEC Tubular Assay Results

For the angiogenesis experiments, the only significant difference between any of the experimental conditions was between the positive LSGS control and the degraded CSC group at a concentration of 100 $\mu\text{g/ml}$. In addition, there was an increase in total tubule length between the positive LSGS control and the degraded groups, but it was not significant. There was also an increase in tubule length for the intact condition, but it was also not significant.

Protocol Development

Following the successful isolation of intact DRGs from a mouse, a live-dead stain was performed to determine the relative viability of the isolation procedure. A representative image of this is shown below in Figure 10.

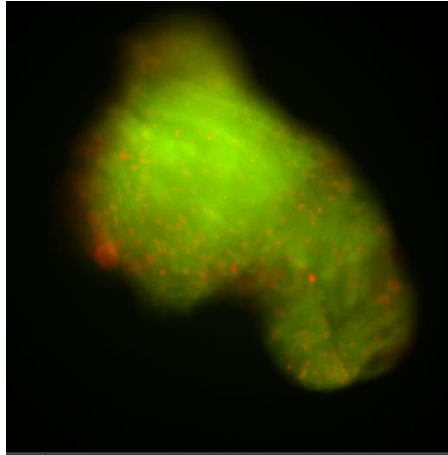


Figure 10: Live-Dead for a Whole Intact DRG

When the intact DRGs are enzymatically digested, and a cell count of viable DRGs is determined utilizing a hemocytometer, the cell count is consistently very low. Figure 12, below, is a representative image demonstrating this.

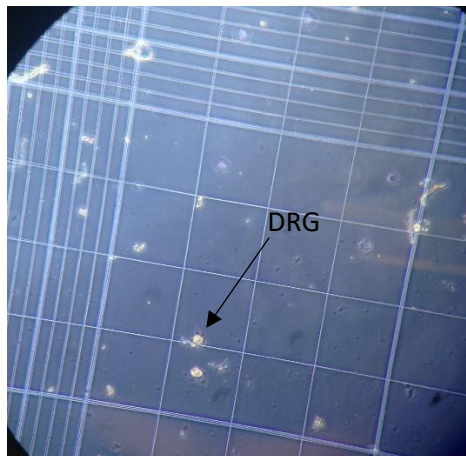


Figure 11: DRG cell count using Hemocytometer

Discussion

Angiogenesis Experiments

The goal of the angiogenesis experiments in this study were to determine the mechanism by which Aggrecan inhibits angiogenesis. Previous literature has shown that intact human Aggrecan inhibits cell adhesion and migration in vitro²³ and that Aggrecan degrades during IVD degeneration²⁴. In addition, a previous study showed that intact and degraded salmon nasal cartilage proteoglycan, which is a member of the Aggrecan family, inhibited angiogenesis in vitro¹⁵.

In our study, we found no inhibition of angiogenesis for any of our groups. This is not surprising, as Aggrecan side chains were utilized for this study rather than whole aggrecan protein. Our experiments also did not include the core protein, which is possibly involved in the inhibitory process. In addition, the representative side-chains chosen for this study were chosen specifically to match those present in human Aggrecan, while those studied by Kobayashi et al were based on availability.

Previous studies have also demonstrated, in some cases, that high concentrations of chondroitin sulfates can have pro-angiogenic affects²⁵, due to their ability to mediate growth factor-mediated migration and morphogenesis. Our results show that in some cases, even degraded chondroitin sulfate can have pro-angiogenic effects. For our high concentration Chondroitin Sulfate-C group, a significant increase in tubular formation can be observed in our degraded condition. The proposed mechanism for this is that degraded chondroitin-sulfate groups contain GAG-peptide fragments, which promote angiogenesis through their supply. Previous research has shown that these released fragments can modulate wound healing in a similar mechanism²⁶.

In addition, the composition of Aggrecan changes as the intervertebral disc ages. Chondroitin 6-Sulfate (CSC) goes from relative low concentrations to dominating the chondroitin sulfate composition¹⁹. This change provides support for the degradation of Chondroitin 6-Sulfate playing a significant role in angiogenesis, as the degradation of adult Aggrecan and its side-chains is typical of IVD degeneration²⁴. These degraded products, namely Chondroitin 6-Sulfate, then produce the angiogenesis that is typical of disease.

This effect becomes especially interesting when combined with data from Kobayashi et al, where they showed that intact salmon Aggrecan inhibits the expression of MMPs, which have been shown to actively degrade Aggrecan in vivo²⁷. This means that when Aggrecan becomes degraded, it loses its inhibition on MMP expression, and simultaneously some of its degraded products promote angiogenesis. In turn, MMPs degrade more Aggrecan, which continues the cycle.

Protocol Development

The protocol modified from Sleight et al, and Dr. Popovich's lab at OSU, improves upon the strengths already present in the procedure, but lack the consistent viability observed in their protocols. The modified protocol improves the speed of dissection time, and it reduces the complexity and difficulty of the dissection by making the DRGs easier to access and extract. Unlike the protocol developed by Sleight et al, our protocol is achievable with a lower quality of surgical tools and has been tested using adult mice. Additionally, the protocol involves steady removal of the spinal cord along with the DRGs, which reduces the amount of time that the DRGs are exposed to air before being extracted and placed in HBSS.

Unfortunately, the protocol developed lacks the consistency of the other protocols developed in their ability to consistently yield viable DRGs. Due to time constraints, a protocol

able to generate consistent viable DRGs was not able to be developed, and this is of definite future interest for this lab.

Significance and Conclusions

The results of this study suggest that the side-chain of Aggrecan most prevalent in adult humans can promote angiogenesis when degraded. This could have significance in determining the mechanism by which angiogenesis, and subsequently, neurogenesis, in the intervertebral disc occurs. An understanding of this process could result in more targeted therapeutics that could reduce the pathogenesis of pain-related processes.

Limitations and Future Work

DRG Cell Viability

The described method of DRG isolation improves on the efficiency and simplicity of previous methodologies, but lacks the ability to generate consistently viable DRG cells. Future work should attempt to manipulate the parameters of the enzymatic digestion protocol, or utilize different digestion enzymes and growth media, as seen in other DRG isolation protocols²⁸.

Angiogenesis Assay

While tubular formation assays are a good indicator of angiogenesis, other assays may be a better indicator. More functional assays, such as cellular migration, or in vivo matrix assays, could provide more insight into the behavior of cells in response to the Chondroitin Sulfate side-chains.²⁹

Future Work

Intact Aggrecan has been shown to inhibit neurogenesis and angiogenesis in vitro, and degradation of that Aggrecan has been shown to arrest that effect^{13,15}. In this study, we found evidence that some degraded chondroitin sulfate chains present on Aggrecan have pro-angiogenic effects, yet we found no evidence that any of the chains studied have an inhibitory effect when left intact. This could be the result of interactions between the side-chains, which could be promoting some effect in the local microenvironment only when they are able to interact. This experiment would remove those effects, as each side-chain is studied in isolation.

References

1. Andersson, G. B. Epidemiological features of chronic low-back pain. *Lancet Lond. Engl.* **354**, 581–585 (1999).
2. Katz, J. N. Lumbar disc disorders and low-back pain: socioeconomic factors and consequences. *J. Bone Joint Surg. Am.* **88 Suppl 2**, 21–24 (2006).
3. Freemont, A. J. *et al.* Nerve ingrowth into diseased intervertebral disc in chronic back pain. *Lancet Lond. Engl.* **350**, 178–181 (1997).
4. Choi, Y.-S. Pathophysiology of Degenerative Disc Disease. *Asian Spine J.* **3**, 39–44 (2009).
5. pmhdev. Herniated Disc - National Library of Medicine. *PubMed Health* Available at: <https://www.ncbi.nlm.nih.gov/pubmedhealth/PMHT0024495/>. (Accessed: 26th March 2018)
6. Intervertebral Disc Process of Degeneration: Physiology and Pathophysiology | Clinical Gate. Available at: <https://clinicalgate.com/intervertebral-disc-process-of-degeneration-physiology-and-pathophysiology/>. (Accessed: 26th March 2018)
7. Raj P. Prithvi. Intervertebral Disc: Anatomy-Physiology-Pathophysiology-Treatment. *Pain Pract.* **8**, 18–44 (2008).
8. Urban, J. P., Maroudas, A., Bayliss, M. T. & Dillon, J. Swelling pressures of proteoglycans at the concentrations found in cartilaginous tissues. *Biorheology* **16**, 447–464 (1979).
9. Maroudas, A., Stockwell, R. A., Nachemson, A. & Urban, J. Factors involved in the nutrition of the human lumbar intervertebral disc: cellularity and diffusion of glucose in vitro. *J. Anat.* **120**, 113–130 (1975).
10. Lotz, J. C., Fields, A. J. & Liebenberg, E. C. The Role of the Vertebral End Plate in Low Back Pain. *Glob. Spine J.* **3**, 153–164 (2013).
11. Purmessur, D. *et al.* Intact glycosaminoglycans from intervertebral disc-derived notochordal cell-conditioned media inhibit neurite growth while maintaining neuronal cell viability. *Spine J. Off. J. North Am. Spine Soc.* **15**, 1060–1069 (2015).
12. Freemont, A. J. *et al.* Nerve growth factor expression and innervation of the painful intervertebral disc. *J. Pathol.* **197**, 286–292 (2002).
13. Johnson, W. E. B. *et al.* Human intervertebral disc aggrecan inhibits nerve growth in vitro. *Arthritis Rheum.* **46**, 2658–2664 (2002).
14. Purmessur, D. *et al.* Intact glycosaminoglycans from intervertebral disc-derived notochordal cell-conditioned media inhibit neurite growth while maintaining neuronal cell viability. *Spine J. Off. J. North Am. Spine Soc.* **15**, 1060–1069 (2015).

15. Kobayashi, T., Kakizaki, I., Nozaka, H. & Nakamura, T. Chondroitin sulfate proteoglycans from salmon nasal cartilage inhibit angiogenesis. *Biochem. Biophys. Rep.* **9**, 72–78 (2017).
16. Kiani, C., Chen, L., Wu, Y. J., Yee, A. J. & Yang, B. B. Structure and function of aggrecan. *Cell Res.* **12**, 19–32 (2002).
17. Gilbert, R. J. *et al.* CS-4,6 is differentially upregulated in glial scar and is a potent inhibitor of neurite extension. *Mol. Cell. Neurosci.* **29**, 545–558 (2005).
18. Gilbert, R. J. *et al.* CS-4,6 is differentially upregulated in glial scar and is a potent inhibitor of neurite extension. *Mol. Cell. Neurosci.* **29**, 545–558 (2005).
19. Collin, E. C. *et al.* Ageing affects chondroitin sulfates and their synthetic enzymes in the intervertebral disc. *Signal Transduct. Target. Ther.* **2**, 17049 (2017).
20. Angiogenesis Analyzer for ImageJ - Gilles Carpentier Research Web Site: Computer Image Analysis. Available at: <http://image.bio.methods.free.fr/ImageJ/?Angiogenesis-Analyzer-for-ImageJ&artpage=2-6>. (Accessed: 28th March 2018)
21. Marquez-Curtis, L. A., Sultani, A. B., McGann, L. E. & Elliott, J. A. W. Beyond membrane integrity: Assessing the functionality of human umbilical vein endothelial cells after cryopreservation. *Cryobiology* **72**, 183–190 (2016).
22. Sleigh, J. N., Weir, G. A. & Schiavo, G. A simple, step-by-step dissection protocol for the rapid isolation of mouse dorsal root ganglia. *BMC Res. Notes* **9**, (2016).
23. Johnson, W. E. B., Caterson, B., Eisenstein, S. M. & Roberts, S. Human intervertebral disc aggrecan inhibits endothelial cell adhesion and cell migration in vitro. *Spine* **30**, 1139–1147 (2005).
24. Iatridis, J. C., Godburn, K., Wuertz, K., Alini, M. & Roughley, P. J. Region-dependent aggrecan degradation patterns in the rat intervertebral disc are affected by mechanical loading in vivo. *Spine* **36**, 203–209 (2011).
25. de Souza Lins Borba, F. K. *et al.* Fractal analysis of extra-embryonic vessels of chick embryos under the effect of glucosamine and chondroitin sulfates. *Microvasc. Res.* **105**, 114–118 (2016).
26. Peplow, P. V. Glycosaminoglycan: a candidate to stimulate the repair of chronic wounds. *Thromb. Haemost.* **94**, 4–16 (2005).
27. Struglics, A. & Hansson, M. MMP proteolysis of the human extracellular matrix protein aggrecan is mainly a process of normal turnover. *Biochem. J.* **446**, 213–223 (2012).
28. de Luca, A. C., Faroni, A. & Reid, A. J. Dorsal root ganglia neurons and differentiated adipose-derived stem cells: an in vitro co-culture model to study peripheral nerve regeneration. *J. Vis. Exp. JoVE* (2015). doi:10.3791/52543

29. Irvin, M. W., Zijlstra, A., Wikswo, J. P. & Pozzi, A. Techniques and assays for the study of angiogenesis. *Exp. Biol. Med. Maywood NJ* **239**, 1476–1488 (2014).